

Palladium(II) and platinum(II) complexes of 2-hydroxy acetophenone *N*(4)-ethylthiosemicarbazone – crystal structure and description of bonding properties

Leuteris Papathanasis^a, Mavroudis A. Demertzis^{a,*}, Paras Nath Yadav^a,
Dimitra Kovala-Demertzi^{a,*}, Christos Prentjas^a, Alfonso Castiñeiras^b,
Stavroula Skoulika^a, Douglas X. West^c

^a Department of Chemistry, University of Ioannina, 45110 Ioannina, Greece

^b Departamento de Química Inorgánica, Universidad de Santiago de Compostela, E-15706 Santiago de Compostela, Spain

^c Department of Chemistry 351700, University of Washington, Seattle, Washington 98195-1700, USA

Received 29 January 2004; accepted 12 June 2004

Available online 28 July 2004

Abstract

Reaction of H_2PtCl_4 and K_2PdCl_4 with 2-hydroxyacetophenone *N*(4)-ethylthiosemicarbazone, $\text{H}_2\text{Ap4Et}$, afforded $[\text{Pt}(\text{Ap4Et})(\text{H}_2\text{Ap4Et})]$ and $[\text{Pd}(\text{Ap4Et})(\text{H}_2\text{Ap4Et})]$. Their crystal and molecular structures are reported and represent the first 1:2 thiosemicarbazone complexes with ligands having both different formal charge and denticity. The dianion, Ap4Et^{2-} , coordinates in a planar conformation to palladium(II) or platinum(II) via the phenolato O, imine N and thiolato S atoms, while the neutral molecule exhibits monodentate coordination by the thione S atom. Intra-, intermolecular hydrogen bonds and $\text{C}-\text{H} \cdots \pi$ contacts lead to aggregation and a supramolecular assembly. Electronic, IR, and NMR spectral data, as well as electrochemical measurements, are included. The $\text{p}K_{\text{a}}$ values of the poorly water soluble $\text{H}_2\text{Ap4Et}$ were obtained spectrophotometrically in aqueous solutions of constant ionic strength.

© 2004 Elsevier B.V. All rights reserved.

Keywords: Palladium(II); Platinum(II); Thiosemicarbazone; Crystal structures; Spectroscopy; Protonation constants

1. Introduction

Thiosemicarbazone derivatives are of considerable interest due to their antibacterial, antimalarial, antiviral and anti-tumor activities [1,2]. In our laboratory, the chemistry of thiosemicarbazones has been an extremely active area of research primarily because of the beneficial biological (viz., antiviral and anti-tumor) activities

of their transition-metal complexes [3–5]. Thiosemicarbazones usually bind to a metal ion as bidentate N,S-donor ligands, when a third donor site (D) is incorporated into the ligands, like Tscs of 2-hydroxyacetophenone, normally D,N,S-tricoordination takes place [6,7]. Examples are also known where such ligands, in addition to displaying D,N,S-tricoordination, bridge a second metal ion through the sulfur [8–10] or oxygen [11–13]. The present report has emerged from our continuous study on the coordination chemistry and on biological activities of Tscs with platinum metals. We report here the structures and spectral properties of $[\text{Pd}(\text{Ap4Et})(\text{H}_2\text{Ap4Et})]$ (2) and $[\text{Pt}(\text{Ap4Et})(\text{H}_2\text{Ap4Et})]$

* Corresponding authors. Tel.: +30265098425; fax: +302650448425.

E-mail addresses: mdemert@cc.uoi.gr (M.A. Demertzis), dkovala@cc.uoi.gr (D. Kovala-Demertzi).

(3), where H_2Ap4Et represents 2-hydroxyacetophenone *N*(4)-ethylTsc, **1**, and $Ap4Et$ the dianion. To our knowledge, this is the first report of 1:2 Tsc complexes with different formal charge and denticity.

2. Experimental

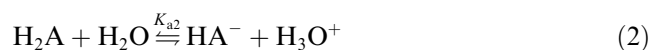
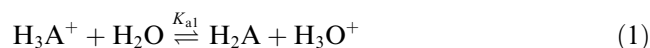
2.1. Materials and physical measurements

Solvents were purified and dried according to standard procedures. Infrared and far-infrared spectra were recorded with a Perkin–Elmer Spectrum GX FT-IR spectrophotometer using KBr pellets ($4000\text{--}400\text{ cm}^{-1}$) and nujol mulls between polyethylene disks ($400\text{--}40\text{ cm}^{-1}$). 1H (250.13 MHz) and ^{13}C (62.90 MHz) NMR spectra were recorded with a Bruker AMX-400 spectrometer at room temperature and referenced to DMSO or $CHCl_3$. UV spectra were recorded on a JASCO V-570 spectrophotometer. **2** and **3** were studied by the extended-Hückel method using the CACAO PC Beta-Version 5.0 package [14]. Electrochemical measurements were made using an AUTOLAB PGSTAT30 potentiostat with a platinum microsphere as working electrode, CHI102 CH Instruments (2 mm diameter), a platinum wire auxiliary electrode and an Ag/AgCl reference electrode in a three electrode configuration. Ferrocene was added at the end of each experiment and used as an internal standard. All potentials are reported relative to ferrocenium/ferrocene (Fe^+/Fc , $E_{1/2} = 0.173\text{ V}$ in DMF); under the experimental conditions used (scan rate 100 mV s^{-1}). Et_4NClO_4 (0.1 M) was used as supporting electrolyte, the solutions were $1 \times 10^{-3}\text{ M}$ in complex, and carried out under a dinitrogen atmosphere.

2.2. Dissociation constants

Due to the low solubility of H_2Ap4Et , as well as its high k_{a1} and low K_{a3} values, spectrophotometry was used to study the dissociation constants. Aqueous H_2Ap4Et solutions of constant ionic strength were prepared with distilled water obtained from a borosilicate autostill BICASA Spa, Model BE-115/R and used to determine dissociation constants by a methodology reported previously [10,15]. A $1 \times 10^{-4}\text{ M}$ stock solution of H_2Ap4Et was initially prepared by suspending the appropriate amount of the compound in a water bath in 0.01 M KOH until dissolution occurred, cooling to room temperature, filling the flask to the required volume with 0.01 M KOH solution and mixing thoroughly. Exactly $5.0 \times 10^{-5}\text{ M}$ working ligand solutions, having different H_3O^+ ion concentrations and constant ionic strength ($\mu = 0.1$), were then prepared with standard HCl or KOH and KCl solutions. All absorption spectra and pH measurements were made at $25\text{ }^\circ\text{C}$ with a Jasco 590 UV/VIS/NIR spectrophotometer guided by a per-

sonal computer and a Methrom 691 pH-meter. H_2Ap4Et possesses two function groups, $-NH$ and $-OH$, with dissociative hydrogens, which undergo two deprotonation steps as a function of pH. For convenience, in this paragraph H_2Ap4Et is designated as H_2A . In aqueous solutions, there are four independent species (i.e., H_3A^+ , H_2A , HA^- and A^{2-}). Thus, there are three separate dissociation steps given by Eqs. (1)–(3)



The law of mass-action for these equations, based on the molar absorptivities of the various species, takes the form,

$$K_{a1} = [H_3O^+] \frac{\epsilon_{H_3A^+} - \epsilon_0}{\epsilon_0 - \epsilon_{H_2A}} \quad (4)$$

$$K_{a2} = [H_3O^+] \frac{\epsilon_{H_2A} - \epsilon_0}{\epsilon_0 - \epsilon_{HA^-}} \quad (5)$$

$$K_{a3} = [H_3O^+] \frac{\epsilon_{HA^-} - \epsilon_0}{\epsilon_0 - \epsilon_{A^{2-}}} \quad (6)$$

respectively. The terms ϵ_0 , $\epsilon_{A^{2-}}$, ϵ_{HA^-} , ϵ_{H_2A} and $\epsilon_{H_3A^+}$ are the molar absorptivities of the observed solution, doubly negative ionized, singly negative ionized, molecular and positively charged species, respectively. In order to find the dissociation constants, the values of the molar absorptivities must be experimentally determined. However, in this particular instance a direct application of relationships (4) and (6) for K_{a1} and K_{a3} determination is impossible, since $\epsilon_{H_3A^+}$ and $\epsilon_{A^{2-}}$ cannot be determined in solutions with ionic strength equal to 0.1. Ideally, A^{2-} and H_3A^+ predominate at very high alkaline or very low

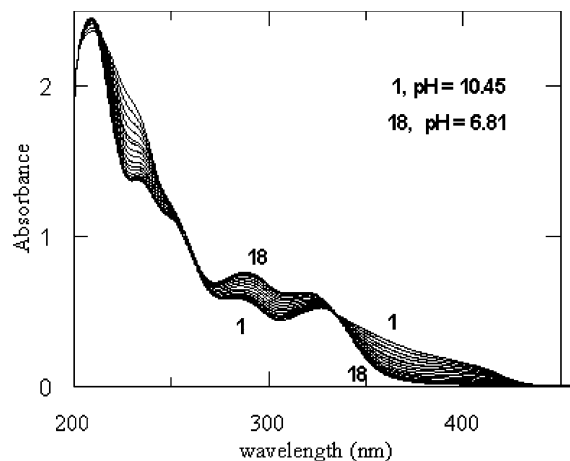


Fig. 1. Electronic absorption spectra of the conjugate pair H_2A – HA^- in the pH region 6.81–10.45.

acid solutions, respectively. Perhaps the equilibrium steps (2) and (3) occur to an extent simultaneously, and the value of the common species HA^- cannot also be determined directly from absorption spectra. Therefore, instead of using relationships (4)–(6), it is expedient to use a proper rearrangement of them in the form,

$$\varepsilon_o = \varepsilon_{\text{H}_3\text{A}^+} - K_{a1} \frac{\varepsilon_o - \varepsilon_{\text{H}_2\text{A}}}{[\text{H}_3\text{O}^+]} \quad (7)$$

$$\varepsilon_o = \varepsilon_{\text{HA}^-} + \frac{1}{K_{a2}} (\varepsilon_{\text{H}_2\text{A}} - \varepsilon_o) [\text{H}_3\text{O}^+] \quad (8)$$

$$\varepsilon_o = \varepsilon_{\text{A}^{2-}} + \frac{1}{K_{a3}} (\varepsilon_{\text{HA}^-} - \varepsilon_o) [\text{H}_3\text{O}^+] \quad (9)$$

respectively [10]. These relationships are useful to find the concentration dissociation constants of the ligand.

2.3. X-ray crystallography

Yellow crystals of **2** and **3** were mounted on glass fibers and used for data collection. Cell constants and an orientation matrix for data collection were obtained by least-squares refinement of 25 reflections in the range $8.919 < \theta < 16.162^\circ$ with a Nonius MACH3 diffractometer for **2** and 21 reflections in the range of $9.73 < \theta < 11.58^\circ$ on a Bruker-P4 diffractometer for **3**. Data were collected at room temperature using the ω -scan technique with Mo $K\alpha$ radiation ($\omega = 0.71073 \text{ \AA}$) at 293 K, corrected for Lorentz and polarization effects, and empirical absorption corrections (ω -scans for **2** and DIFABS for **3**) were made [16]. The structures were solved by direct methods and subsequent difference Fourier maps, and refined on F^2 by a full-matrix least-squares procedure using anisotropic displacement parameters [17]. Hydrogen atoms were located in their calculated positions (C–H 0.93–0.97 \AA) and were refined using a riding model. The O–H and N–H hydrogen atoms were initially positioned at site determined from difference maps and allowed to refine using, respectively, the AFIX-148 and AFIX-48 controls in SHELXL-97. Atomic scattering factors are from “International Tables for X-ray Crystallography” [18]. Drawings were made using PLATON [19].

2.4. Preparation of compounds

$\text{H}_2\text{Ap4Et}$ (**1**) was prepared by reacting equimolar amounts of 2-hydroxyacetophenone (2 mmol) and ethyl thiosemicarbazide (2 mmol) in 10 ml methanol as described in the literature [8].

$[\text{Pd}(\text{Ap4Et})(\text{H}_2\text{ApEt})]$ (**2**) was synthesized by reacting **1** (0.8 mmol) in 10 methanol with an aqueous solution of K_2PdCl_4 (0.4 mmol). The pH of the solution was adjusted to 9.0–9.5 by addition of aqueous NH_3 and the reaction mixture stirred for 24 h at room tem-

perature. The resulting light yellow powder was filtered off, washed with cold methanol and ether and dried in vacuo over silica gel, finally redried at 70°C in vacuo over P_4O_{10} ; decomposition point 206°C , yield 42%. IR (KBr): 1580 $\nu(\text{C}=\text{N})$, 1563 $\nu(\text{C}=\text{N})$, 810 $\nu(\text{C}=\text{S})$, 748 $\nu(\text{C}-\text{S})$, 481 $\nu(\text{Pd}-\text{N})$, 353 and 325 $\nu(\text{Pd}-\text{S})$, 445 $\nu(\text{Pd}-\text{O})$; Elemental analyses are consistent with $\text{C}_{22}\text{H}_{28}\text{N}_6\text{O}_2\text{S}_2\text{Pd}$ (Calc.: C, 45.6; H, 4.8; N, 14.5; S, 11.2. Found: C, 45.8; H, 5.1; N, 14.8; S, 11.2%).

$[\text{Pt}(\text{Ap4Et})(\text{H}_2\text{Ap4Et})]$ (**3**) was prepared from the reaction of **1** (0.8 mmol) in ethanol (10 ml) with the stock solution of PtCl_4^{2-} (20 ml, 0.4 mmol). A stock PtCl_4^{2-} solution was prepared by dissolving PtCl_2 (2.66 g, 10 mmol) in concentrated HCl under reflux, filtering to remove the turbidity caused by undissolved material, neutralizing with Na_2CO_3 and diluting with distilled water up to 250 mL (pH 6.0–6.5) to yield a solution of 0.04 M Na_2PtCl_4 . The pH of the reaction solution was adjusted to 9.0–10.0 with aqueous NEt_3 , and the reaction mixture stirred for 3 days at room temperature. The yellow powder was filtered off, washed with cold ethanol and ether and dried as above; decomposition point 222°C , yield 60%. IR(KBr): 1581 $\nu(\text{C}=\text{N})$, 1561 $\nu(\text{C}=\text{N})$, 811 $\nu(\text{C}=\text{S})$, 748 $\nu(\text{C}-\text{S})$, 479 $\nu(\text{Pt}-\text{N})$, 352 and 339 $\nu(\text{Pt}-\text{S})$, 442 $\nu(\text{Pt}-\text{O})$; Elemental analyses are consistent with $\text{C}_{22}\text{H}_{28}\text{N}_6\text{O}_2\text{S}_2\text{Pt}$ (Calc.: C, 39.6; H, 4.3; N, 12.6; S, 9.6. Found: C, 40.0; H, 4.2; N, 11.9; S, 10.6%). Slow evaporation of dilute DMF solutions of **2** and **3** provided yellow crystals suitable for X-ray structural analysis.

3. Results and discussion

3.1. Dissociation constants

The concentration dissociation constants of **1** were determined and the 95% confidence limits of their logarithms were found to be equal to $\text{p}K_{a1} = 1.75 \pm 0.02$, $\text{p}K_{a2} = 8.81 \pm 0.04$ and $\text{p}K_{a3} = 12.96 \pm 0.01$. $\text{p}K_{a1}$ is assigned to the dissociation of the protonated Tsc moiety by comparison with protonated thiosemicarbazide, $\text{p}K_a = 1.70\text{--}1.87$ [20], $\text{p}K_{a2}$ to the hydroxyl group by comparison with acetylphenol, $\text{p}K_a = 9.89\text{--}9.94$ [20] and $\text{p}K_{a3}$ to the thiol/thioamide group. The replacement of the N(2)-hydrogen in a Tsc moiety by a methyl group prevents the observation of the third dissociation constant adding credence to our assignment [21]. The relative standard deviation of the slopes, their confidence limits, the correlation coefficients, the analytical wavelengths and the $\text{p}K_a$ s of the above relationships are shown in Table 1. In aqueous solutions in the pH region from 1.62 to 12.81, there are four independent species (i.e., H_3A^+ , H_2A , HA^- and A^{2-}) and two of them are shown by the electronic absorption spectra in Fig. 1.

Table 1
Analytical parameters of calibration graphs for acid–base properties of **1**

RSD of slope (%)	Confidence limit of slope	Correlation coefficient	Wavelength λ (nm)	pK_a
2.87	$-1.79 \times 10^2 \pm 8.10 \times 10^{-4a}$	0.9989	287	$pK_{a1} = 1.79$
3.28	$6.51 \times 10^8 \pm 7.30 \times 10^{7b}$	0.9934	308	$pK_{a2} = 8.81$
4.66	$-9.20 \times 10^{12} \pm 1.48 \times 10^{10c}$	0.9999	285	$pK_{a3} = 12.96$

^a $n = 9$.

^b $n = 9$.

^c $n = 7$.

3.2. Synthesis

The interaction of K_2PdCl_4 and H_2PtCl_4 with **1** in basic solution (pH ca. 9) and 1:2 molar ratio afforded the complexes **2** and **3**, Scheme 1.

However, two other complexes have been obtained by the reaction of Li_2PdCl_4 in methanol or aqueous K_2PdCl_4 with **1** by using different molar ratios and changing the pH. The mononuclear complex $[Pd(HA-p4Et)Cl]$ is prepared in methanol (1:1 molar ratio) and $[Pd(Ap4Et)_3]$ in the pH range of 9–10 (1:1 molar ratio). $[Pd(Ap4Et)_3]$ can also be formed from the monomer on dissolution in DMF or directly from Li_2PdCl_4 and **1** in methanol–ammonia solution [8]. When Na_2PtCl_4 reacts with **1** in methanol or aqueous solutions using different molar ratios and pH values, **3** is the only product formed.

3.3. Molecular structures

Perspective views of **2** and **3** with the atomic numbering schemes are shown in Figs. 2 and 3, respectively and crystal data are given in Table 2, together with refinement details. Selected bond distances and angles are listed in Table 3.

The ligands are not equivalent, one being dianionic and tridentate with O,N,S donation; the other ligand is neutral and monodentate using only the sulfur atom, S(2), to coordinate to the metal. The coordination environment, MONSS, is essentially planar with a maximum deviation from the least-squares plane of 0.058(2) Å for N(22) and 0.060(1) Å for N(21) for **2** and **3**, respectively. The dianionic, tridentate ligand has a ZEZ

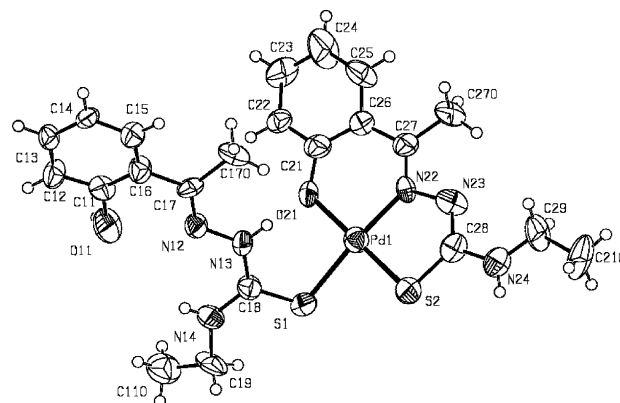


Fig. 2. ORTEP diagram of **2** with the labeling scheme.

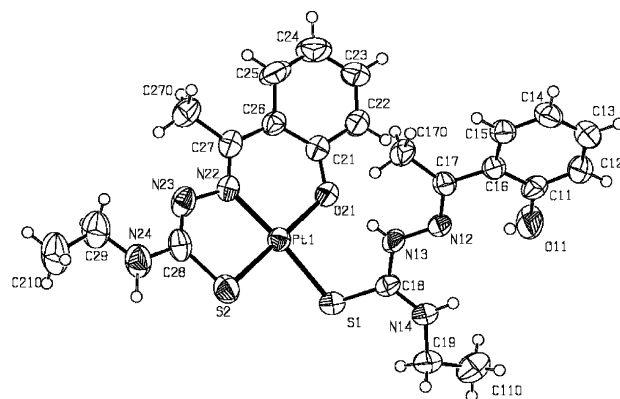
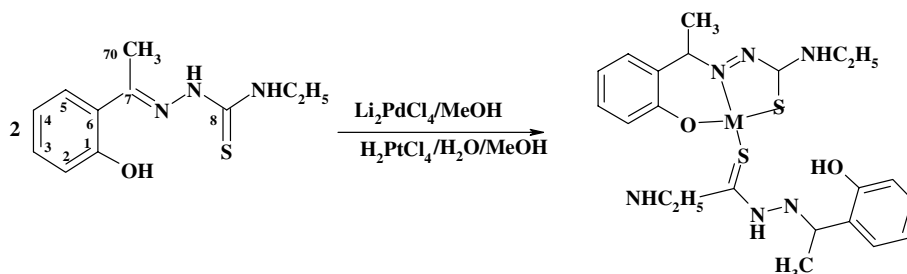


Fig. 3. ORTEP diagram of **3** with the labeling scheme.



Scheme 1. The reaction path for the synthesis of **2** and **3**.

Table 2
Crystal data, data collection and structure refinement

Compound	2	3
Formula	C ₂₂ H ₂₈ N ₆ O ₂ PdS ₂	C ₂₂ H ₂₈ N ₆ O ₂ PtS ₂
Formula weight	579.02	665.70
Crystal system	triclinic	triclinic
Space group	$P\bar{1}$	$P\bar{1}$
<i>a</i> (Å)	7.2792(8)	7.336(2)
<i>b</i> (Å)	13.475(3)	13.508(2)
<i>c</i> (Å)	13.506(2)	13.567(2)
α (°)	73.607(19)°	73.350(10)°
β (°)	83.608(13)°	74.5900(10)°
γ (°)	75.251(13)°	83.380(10)°
<i>V</i> (Å ³)	1227.9(4)	1240.6(4)
<i>Z</i>	2	2
<i>D</i> _x (g cm ⁻³)	1.566	1.782
<i>F</i> (000)	592	652
μ (mm ⁻¹)	0.957	5.854
Crystal size (mm)	0.20 × 0.25 × 0.10	0.20 × 0.10 × 0.15
θ range (°)	3.96–24.64	1.93–25.00
<i>hkl</i> Range	8 ≤ <i>h</i> ≤ 0 –15 ≤ <i>k</i> ≤ 15 –15 ≤ <i>l</i> ≤ 15	0 ≤ <i>h</i> ≤ 8 –14 ≤ <i>k</i> ≤ 14 –14 ≤ <i>l</i> ≤ 14
Reflections collected	4448	4555
Reflections unique (<i>R</i> _{int})	4093 (0.1014)	4216 (0.0377)
Data/restraints/parameters	4093/0/299	4216/0/299
Extinction coefficient	0.0031(18)	
Final <i>R</i> indices	<i>R</i> ₁ = 0.0546, <i>wR</i> ₂ = 0.1050	<i>R</i> ₁ = 0.0434, <i>wR</i> ₂ = 0.0978
<i>R</i> indices (all data)	<i>R</i> ₁ = 0.1884, <i>wR</i> ₂ = 0.1615	<i>R</i> ₁ = 0.0583, <i>wR</i> ₂ = 0.1050
Goodness-of-fit	0.944	1.033
max/min $\Delta\rho$ (e Å ⁻³)	0.031 and –0.029	0.836 and –1.049

Table 3
Selected bond distances (Å) and angles (°) for 2 and 3

2		3	
Pd(1)–N(21)	1.9681(14)	Pt(1)–N(21)	2.007(6)
Pd(1)–O(21)	1.9946(15)	Pt(1)–O(21)	2.008(6)
Pd(1)–S(2)	2.2281(15)	Pt(1)–S(2)	2.238(2)
Pd(1)–S(1)	2.3213(14)	Pt(1)–S(1)	2.317(2)
S(1)–C(18)	1.6582(14)	S(1)–C(18)	1.711(9)
S(2)–C(28)	1.7346(15)	S(2)–C(28)	1.771(10)
O(11)–C(11)	1.3528(14)	O(11)–C(11)	1.358(11)
O(21)–C(21)	1.3596(15)	O(21)–C(21)	1.329(9)
N(11)–C(17)	1.2284(14)	N(11)–C(17)	1.297(10)
N(11)–N(12)	1.4096(14)	N(11)–N(12)	1.377(9)
N(12)–C(18)	1.3431(14)	C(18)–N(12)	1.350(10)
N(13)–C(18)	1.3514(15)	C(18)–N(13)	1.311(10)
N(13)–C(19)	1.4528(14)	N(13)–C(19)	1.462(11)
N(21)–C(27)	1.2876(15)	N(21)–C(27)	1.298(10)
N(21)–N(22)	1.4206(14)	N(21)–N(22)	1.400(9)
N(22)–C(28)	1.3281(15)	N(22)–C(28)	1.278(12)
N(23)–C(28)	1.3612(15)	N(23)–C(28)	1.366(11)
N(23)–C(29)	1.3938(15)	N(23)–C(29)	1.456(12)
N(21)–Pd(1)–O(21)	92.46(2)	N(21)–Pt(1)–O(21)	93.4(2)
N(21)–Pd(1)–S(2)	87.65(2)	N(21)–Pt(1)–S(2)	86.4(2)
O(21)–Pd(1)–S(2)	178.335(7)	O(21)–Pt(1)–S(2)	178.40(18)
N(21)–Pd(1)–S(1)	173.897(7)	N(21)–Pt(1)–S(1)	174.4(2)
O(21)–Pd(1)–S(1)	91.43(2)	O(21)–Pt(1)–S(1)	90.33(17)
S(2)–Pd(1)–S(1)	88.599(19)	S(2)–Pt(1)–S(1)	90.00(9)

configuration based on the C(11)–C(16), N(12)–C(17) and N(13)–C(10) bonds, while the monodentate ligand shows an EEZ configuration with respect to the same bonds. These structures with tridentate/monodentate bonding, rather than bis-bidentate, result from the preferential binding of sulfur over nitrogen to palladium(II) and platinum(II), the high stability of the tricyclic ring system of the tridentate ligand and the tendency of the ligands to retain planar structures. The ligand planarity is indicated by the dihedral angle between the mean planes of the phenol ring and M–S–C–N–N and the mean planes of the phenol ring and the M–N–C–C–C–O, 2.89(2) and 0.69(2)°, respectively, for **2** and 4.24(2) and 2.86(2)° for **3**. The negative charge of the dianionic ligand is delocalized over the Tsc moiety and the S–C bond distances are consistent with increased single bond character, while the imine C–N distances and both thioamide C–N distances indicate considerable double bond character (Table 2). The S–C bond distances for the monodentate ligand are consistent with double bond character, indicating a neutral molecule in the thione form, protonated on N(13). The bond distances O(21)–C(21) and O(11)–C(11) are indicative of a single bond, shortened by the neighborhoods of the phenyl ring, as expected for protonated O(11) and metallated O(21) oxygens (Table 3). The M–O, M–N and M–S bond distances are similar to those found in other palladium(II) and platinum(II) complexes [9,22]. The monomers of **2** and **3** form hydrogen-bonded dimers linked by two N(14)–H···S(2) hydrogen bonds, involving the N(14)H hydrogen atom of the monodentate ligand and the adjacent sulfur atom S(2) of the tridentate ligands and vice versa of centro-symmetrically related pairs of molecules. The observed hydrogen-bonding pattern is

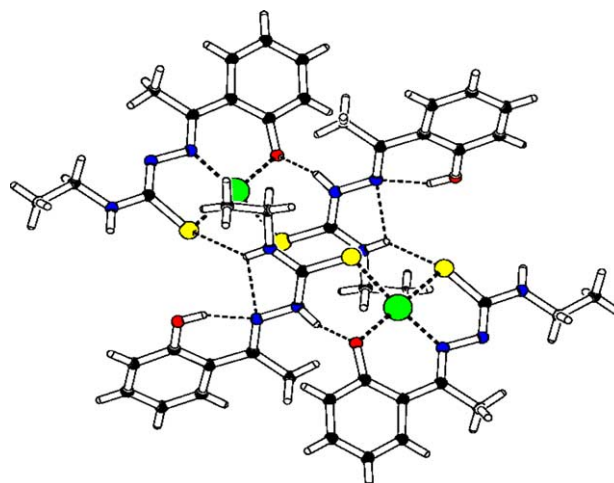


Fig. 4. Intra- and intermolecular hydrogen bonds of **3**.

of the DA = AD type. N(13)–H intramolecularly hydrogen bonds to coordinated O(21) and intermolecularly to S(2) in **2** and **3** (Fig. 4).

The crystal packing is determined by C–H → π interactions, which are listed in Table 4 and shown in the packing diagram in Fig. 5.

3.4. Spectroscopy

The ^1H NMR spectrum of **1** shows two signals for OH, 10.77, 12.60 ppm, and NH, 8.63, 8.33 ppm, which is consistent with about one-third of the mixture being the O–H···N hydrogen bonding isomer [11–13]. Two sets of peaks are also present for a number of the hydrogen and carbon atoms of **1** consistent with two isomers and **2** and **3** also show two sets of peaks because of dif-

Table 4
Intra- and intermolecular hydrogen bonding and C–H– π stacking interactions for **2** and **3**^a

2					3				
Donor D	Acceptor A	H···A	D···A	D–H···A	Donor D	Acceptor A	H···A	D···A	D–H···A
N(13)	O(21)	2.246	2.746(4)	121.61	O(11)	N(12)	2.1020	2.613(11)	148.50
N(14)	N(12)	2.3365	2.682(4)	104.31	N(13)	O(21)	2.3564	2.801(9)	120.81
N(14)	S(2) ⁱ	2.7795	3.488(3)	140.69	N(14)	N(12)	2.2324	2.639(11)	105.59
C(12)	O(11) ⁱⁱ	2.5756	3.471(4)	161.78	N(14)	S(2) ^{xii}	2.7845	3.515(8)	136.29
C(15)	O(21) ⁱⁱⁱ	2.5448	3.439(5)	161.37	C(110)	S(2) ^{xiii}	2.8161	3.667(13)	148.28
					C(15)	O(21) ⁱⁱⁱ	2.6707	3.103(10)	107.50
		H···Cg	X···Cg	C–H···Cg			H···Cg	X···Cg	C–H···Cg
C(110)	Cg(3) ^{iv}	2.981	3.889	158.18	C(110)	Cg(3) ^{iv}	2.986	3.851	150.42
C(210)	Cg(3) ^v	2.886	3.832	168.93	C(210)	Cg(3) ^{viii}	2.997	3.914	159.98
C(270)	Cg(2) ^{vi}	3.008	3.836	145.32	C(270)	Cg(1) ^{ix}	2.926	3.717	140.50
C(270)	Cg(1) ^{vii}	2.708	3.597	154.18	C(270)	Cg(2) ^x	2.932	3.848	159.91
C(29)	Cg(4) ^{viii}	2.783	3.666	151.70	C(29)	Cg(4) ^{ix}	2.709	3.621	156.92

Symmetry operations; *i*: 1–*x*, –*y*, –1–*z*; *ii*: 2–*x*, –1–*y*, –1–*z*; *iii*: 1+*x*, *y*, *z*; *iv*: –1+*x*, *y*, *z*; *v*: –1+*x*, 1+*y*, *z*; *vi*: 1–*x*, –*y*, –*z*; *vii*: –*x*, –*y*, –*z*; *viii*: 1+*x*, *y*, 1+*z*; *ix*: –1–*x*, 2–*y*, 1–*z*; *x*: –*x*, 2–*y*, 1–*z*; *xi*: –*x*, 1–*y*, 1–*z*; *xii*: –1–*x*, 1–*y*, 1–*z*.

^a Cg(1) and Cg(2) are the centroids of the rings M(1)–S(2)–N(22)–N(23) and M(1)–O(21)–N(22)–C(21)–C(26)–C(27), respectively, where M is Pd or Pt; Cg(3) and Cg(4) are the centroids of the phenyl rings C(11)–C(12)–C(13)–C(14)–C(15)–C(16) and C(21)–C(22)–C(23)–C(24)–C(25)–C(26), respectively.

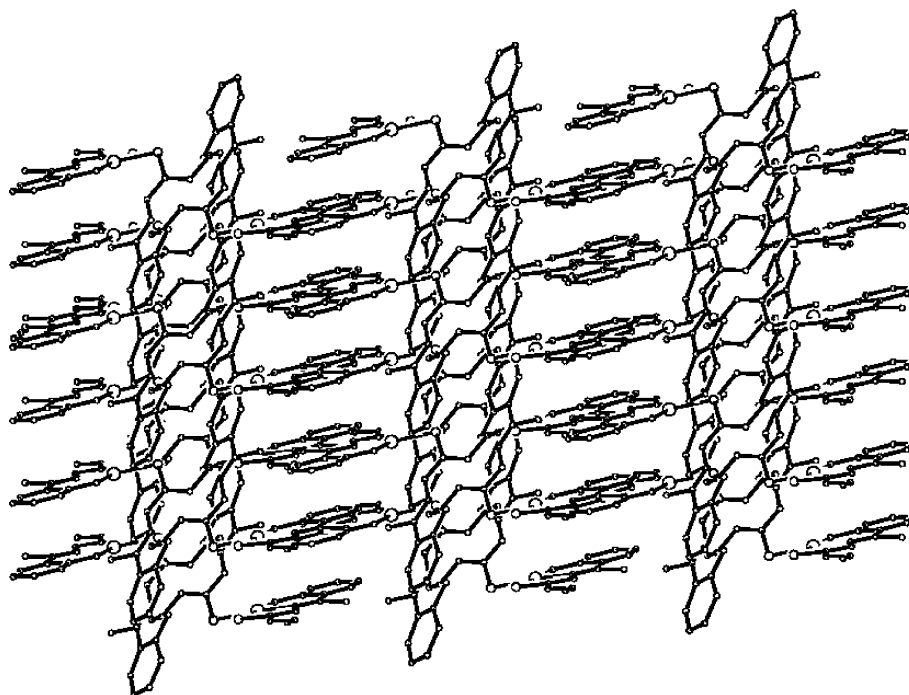


Fig. 5. A view of the extended network of the intermolecular hydrogen bonds in **2** along the *b* axes.

ferent bonding of the ligands. Comparison of the ^1H NMR spectra of **2** and **3** with the spectrum of **1** shows small upfield shifts for C(3)H, C(4)H and C(5)H, indicating increased electron density at these sites on complexation. These shifts, as well as downfield shifts for C(2)H and C(70)H₃, result from coordination of the phenoxy oxygen and imine nitrogen atoms. Downfield shifts are also observed for the imine carbon, C(7) indicating decreased electron density on coordination. How-

ever, C(8) is shifted upfield considerably in the spectra of **2** and **3** due to greater back π -bonding for thiolato function than the imine function.

The electronic absorption spectra of **1–3** exhibit bands at *ca.* 300 and 330 nm and of **2–3** do have a shoulder at 400–420 nm. The absorptions in the ultraviolet region are assignable to transitions within the ligand orbitals and that in the visible region is probably due to charge transfer transition involving metal and ligand

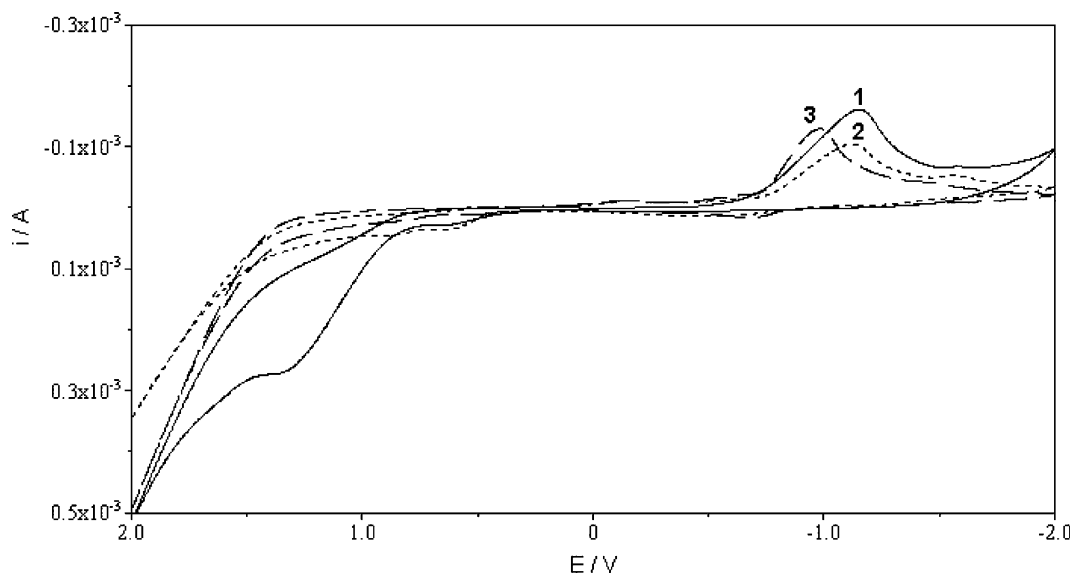


Fig. 6. Cyclic voltammograms (100 mV s^{-1}) of **1–3** in DMF (1.0 mM) in the range +2.0–2.0 V. The quoted potentials are vs. ferrocene/ferrocenium.

orbitals [22]. For a better understanding of the nature of the transition in the visible region, qualitative EHMO calculations have been performed using the crystallographic coordinates for **2** and **3**. The highest occupied molecular orbital (HOMO) of **2** is composed of d_{xz} , d_{yz} and $d_{x^2-y^2}$ orbitals from palladium and the HOMO of **3** has a major contribution from the d_{xz} , d_{yz} and d_{xy} orbitals from platinum. The lowest unoccupied molecular orbital (LUMO) of **2** and **3** is entirely localized on different parts of the thiosemicarbazone ligands. The HOMO energy is isolated, suggesting that the assignment of the lowest energy electronic transition can be assigned to the computed HOMO-LUMO. Hence, the absorption in the visible region may be assigned to charge transfer transition occurring from the filled d orbitals of palladium or platinum to the vacant π^* orbitals of the thiosemicarbazone ligands.

Cyclic voltammetry in anhydrous DMF solution shows that **1** exhibits an irreversible reduction peak at -1.145 V, probably corresponding to reduction of the Tsc moiety. **2** and **3** show irreversible reductions at -1.114 and -0.9802 V, respectively. The electrochemical data suggest that the reduction of **2** and **3** might be regarded as being more or less centered on the ligand system. The electron transfers from the platinum cathode and is directed to the π^* LUMO orbital of thiosemicarbazone ligand (Fig. 6) [23,7].

4. Supplementary material

Crystallographic data, i.e., atomic coordinates, thermal parameters, bond lengths and bond angles for **2** and **3**, CCDC Nos. 182923 and 182924, respectively, have been deposited with the Cambridge Crystallographic Data Centre as supplementary publication no. CCDC-1003/m. Copies of available material can be obtained, free of charge, on application to CCDC, 12 Union Road, Cambridge CB2 1EZ, UK, (fax: +44 1223 336033 or e-mail: deposit@ccdc.cam.ac.uk).

Acknowledgments

P.N.Y. thanks I.K.Y. for a scholarship and L.P. thanks E.P.E.A.E.K. of Bioinorganic Chemistry for a scholarship. M.A.D. and D.K.D. thank the Research

Committee of University of Ioannina, Professor S. Dakaris, for in part funding of this research.

References

- [1] H. Beraldo, D. Gambino, *Mini Rev. Med. Chem.* 4 (2004) 159.
- [2] A. Gómez Quiroga, C. Navarro Ranninger, *Coord. Chem. Rev.* 248 (2004) 119.
- [3] D. Kovala-Demertzi, M.A. Demertzis, V. Varagi, A. Papageorgiou, D. Mourelatos, E. Mioglou, Z. Iakovidou, A. Kotsis, *Chemotherapy* 44 (1998) 421.
- [4] T. Varadinova, D. Kovala-Demertzi, M. Rupelieva, M.A. Demertzis, P. Genova, *Acta Virol.* 45 (2001) 87.
- [5] Z. Iakovidou, A. Papageorgiou, M.A. Demertzis, E. Mioglou, D. Mourelatos, A. Kotsis, P.N. Yadav, D. Kovala-Demertzi, *Anti-cancer Drugs* 12 (2001) 65.
- [6] I. Pal, F. Basuli, T.C.W. Mak, S. Bhattacharya, *Angew. Chem., Int. Ed. Engl.* 40 (2001) 2923.
- [7] S. Dutta, F. Basuli, S.-M. Peng, G.-H Lee, S. Bhattacharya, *New J. Chem.* 26 (2002) 1607.
- [8] D. Kovala-Demertzi, N. Kourkoumelis, D.X. West, J. Valdés-Martínez, S. Hernández-Ortega, *Eur. J. Inorg. Chem.* (1998) 861.
- [9] D. Kovala-Demertzi, N. Kourkoumelis, M.A. Demertzis J.R. Miller, C.S. Frampton, J.K. Swearingen, D.X. West, *Eur. J. Inorg. Chem.* (2000) 727.
- [10] P.N. Yadav, M.A. Demertzis, D. Kovala-Demertzi, A. Castineiras, D.X. West, *Inorg. Chim Acta* 332 (2002) 204.
- [11] Z. Lu, C. White, A.L. Rheingold, R.H. Crabtree, *Inorg. Chem.* 32 (1993) 3991.
- [12] D.X. West, Y.-H. Yang, T.L. Klein, K.I. Goldberg, A.E. Liberta, J. Valdés-Martínez, R.A. Toscano, *Polyhedron* 14 (1995) 1681.
- [13] D.X. West, Y.-H. Yang, T.L. Klein, K.I. Goldberg, A.E. Liberta, J. Valdés-Martínez, S. Hernández-Ortega, *Polyhedron* 14 (1995) 3051.
- [14] C. Mealli, D. Proserpio, CACAO PC Beta-Version 5.0, 1998.
- [15] A. Demertzis, S.K. Hadjikakou, D. Kovala-Demertzi A. Koutsodimou, M. Kubicki, *Helv. Chim. Acta* 83 (2000) 2787.
- [16] B.V. Nonius, CAD4-Express Software, Ver. 5.1/1.2. Enraf Nonius, Delft, The Netherlands, 1994.
- [17] G.M. Sheldrick, SHELXL-97, Program for the Refinement of Crystal Structures, University of Göttingen, Germany, 1997.
- [18] International Tables for X-ray Crystallography, vol. C, Kluwer Academic Publishers, Dordrecht, The Netherlands, 1995.
- [19] A.L. Spek, PLATON, A Multipurpose Crystallographic Tool, Utrecht University, Utrecht, The Netherlands, 2001.
- [20] A.E. Martell, R.M. Smith *Critical Statistical Constants*, vol. 4, Plenum Press, New York, 1977.
- [21] E.W. Ainscough, A.M. Brodie, W.A. Denny, G.J. Finlay J.D. Ranford, *J. Inorg. Biochem.* 70 (1998) 175.
- [22] A.B.P. Lever, *Inorganic Electronic Spectroscopy*, Elsevier, New York, 1984.
- [23] J.A. Weinstein, N.N. Zheligovskaya, M.Ya. Me'nikov, F. Hartl, *J. Chem. Soc., Dalton Trans.* (1998) 2459.